

We are IntechOpen, the world's leading publisher of Open Access books Built by scientists, for scientists

6,900

Open access books available

186,000

International authors and editors

200M

Downloads

Our authors are among the

154

Countries delivered to

TOP 1%

most cited scientists

12.2%

Contributors from top 500 universities



WEB OF SCIENCE™

Selection of our books indexed in the Book Citation Index
in Web of Science™ Core Collection (BKCI)

Interested in publishing with us?
Contact book.department@intechopen.com

Numbers displayed above are based on latest data collected.
For more information visit www.intechopen.com



Slow Electromagnetic Waves: Theory and New Applications

Giuseppe Di Massa

Additional information is available at the end of the chapter

<http://dx.doi.org/10.5772/66672>

Abstract

In this chapter, the usage of slow electromagnetic waves in several application domains is deeply discussed. Starting from an outline of the classical Cerenkov effect, various related topics are presented in detail, namely the generation of electromagnetic waves by the Cerenkov effect, the Cerenkov free-electron laser, pickup and kickers in accelerators, pulse compression in radar and linac, and compact components and waveguides in the microwave region.

Keywords: slow electromagnetic waves, propagation, pulse compression, electron beam pickup and kicker

1. Introduction

The pioneering work of Pavel Alekseyevich Cerenkov [1] reports the existence of a visible radiation from pure liquids and solids when electrons go through the medium with a velocity greater than that of light. The radiation, not observed until then, had characteristics that the physical processes responsible for its production were not any of the usual ones associated with atomic or molecular changes. During his studies Cerenkov showed that the radiation was not fluorescent, and that it was polarized with the electric vector parallel to the direction of the electron beam. In a later work [2], he showed that the radiation depended uniquely on the refractive index of the medium and had the unusual property of being emitted asymmetrically.

In [3], a theoretical explanation has been given on this phenomenon which is entirely classical, but in agreement with the qualitative observations of Cerenkov. A striking feature of this theory is that it describes a new process for the production of radiation.

In recent years, the research interest in Cherenkov radiation has arisen due to progress in its new applications such as biomedical imaging, photonic structures, metamaterials, and beam

physics. These new applications require Cherenkov radiation theory of short bunches to be extended to rather more complicated media and structures.

The effect of Cherenkov electromagnetic radiation is similar to that of a sonic boom when an object moves faster than the speed of sound; in this case, the radiation is a shock wave set up in the electromagnetic field.

In this chapter, we report techniques for the excitation of slow waves in guiding structures highlighting classic and new applications, namely:

- Generation of electromagnetic waves by the Cherenkov effect;
- Cherenkov free-electron laser;
- Pickup and kickers in accelerators;
- Pulse compression in radar and linac;
- Compact components and waveguides in microwave region.

2. Outline of Cherenkov radiation

We consider a charged particle traveling at a uniform velocity in a dielectric medium and the electromagnetic field close to the particle that polarizes the medium along its track.

In this process, the atoms are not excited by the charged particle and neither are they removed from their bound states (ionization). It is true that there is in addition ionization, when the impacts are sufficiently close, but the process with which we are concerned here arises from only very small displacements by a very large number of electrons.

Now, when the particle is slow, less than the velocity of light in the considered medium, the radiation from these displaced electrons is not observed, owing to destructive interference. If, however, the velocity of the particle in the medium is faster than the phase velocity of light in the medium, the waves are in phase with one another on a wavefront inclined to the direction of the track, and a coherent electromagnetic radiation is then observed.

If a particle travels a distance AB (**Figure 1**) inside a dielectric medium [4], at a high velocity βc , where c is the velocity of light in a vacuum, and we denote, as sources of spherical waves, the points P_1, P_2, P_3 , then the resulting wave front will lie along the line BC , and the direction of emission of the radiation will be along the line AC , at right angles to BC . The distance the particles travels, in a time Δt , will be $AB = \beta c \Delta t$; at the same time, the waves will have traveled a distance $AC = (c/n)\Delta t$ where n is the refractive index of the medium. From these relations, we obtain

$$\cos \theta = \frac{1}{\beta n} \quad (1)$$

Eq. (1) is a fundamental relation between the velocity of the particle, the refractive index of the medium, and the angle at which the light is emitted. This relation is known as the Cherenkov relation.

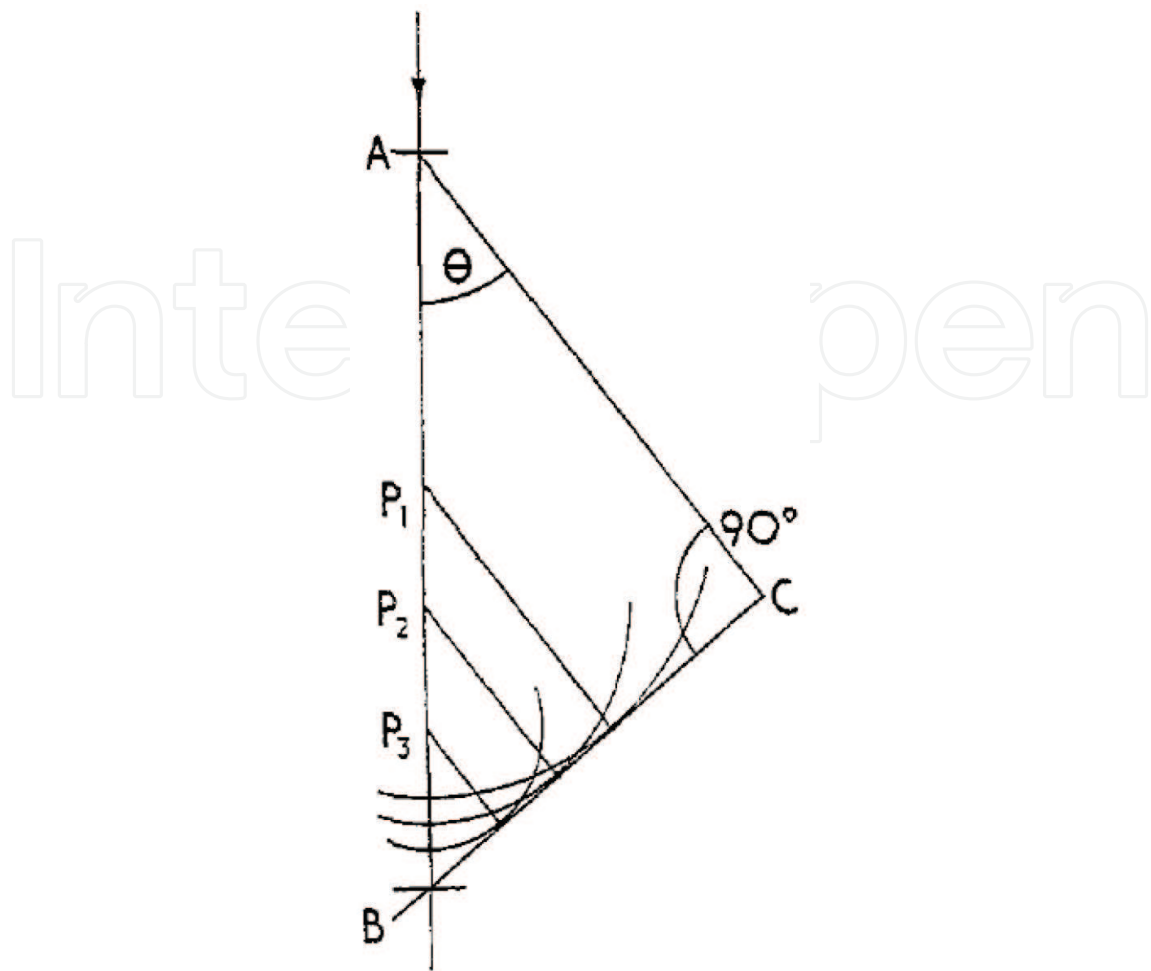


Figure 1. The coherent nature of Cerenkov radiation.

The quantity β is related to the kinetic energy E of the particle, and to its rest mass m , by the equation:

$$E = mc^2 \left[\frac{1}{\sqrt{1-\beta^2}} - 1 \right] \quad (2)$$

Two special conditions are included in Eq. (1) for limiting cases. First, there is a threshold condition, namely when $\beta = 1/n$ and $\theta = 0$. This implies a kinetic energy for the particle below which no radiation takes place. Second, there is a maximum angle at which the light may be emitted, when the particle is traveling at ultrarelativistic velocities. This arises when $\beta \rightarrow 1$, in which case $\theta_{\max} \rightarrow \cos^{-1}(1/n)$.

The situation depicted in **Figure 1** has been drawn in one plane. In practice, the light is emitted over a conical surface, the axis of which coincides with that of the particle, and the semiapex angle of which is the angle θ , which is shown in **Figure 2**. The polarization of the electric vector E is always at right angles to the direction of propagation of the light, and the magnetic vector H is always tangential to the surface of the cone, as shown in **Figure 2**.

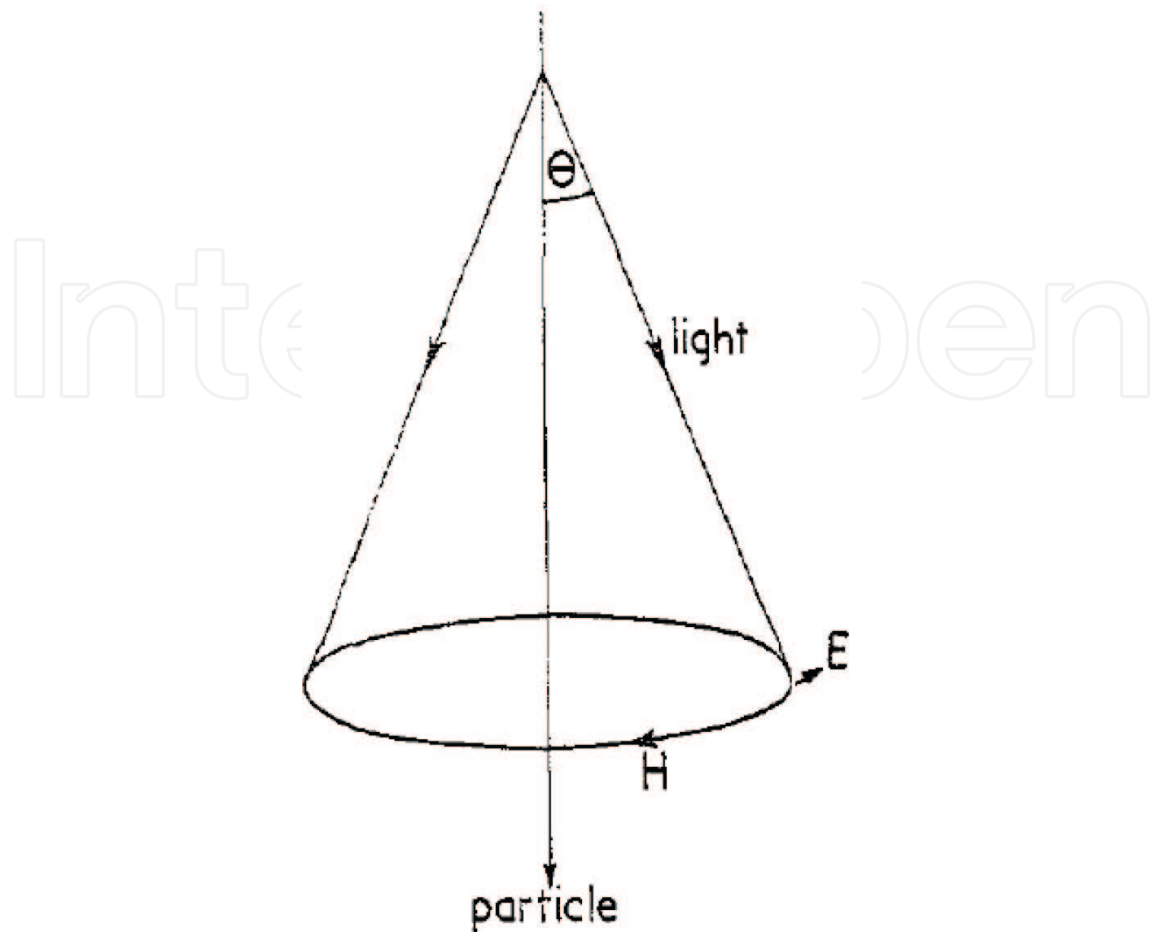


Figure 2. Cerenkov cone of radiation.

3. Cerenkov radiation in the microwave region

A charged particle of velocity v is a potential source of electromagnetic waves which has an infinite and uniform spectrum [5]. It is well known that if it is traveling in an infinite dielectric medium of index of refraction $n(f)$, function of frequency f , we get an electromagnetic radiation for all frequencies satisfying the following equation:

$$n(f)v > 1 \quad (3)$$

So we have conical waves at which have an angle ϑ with respect to the axis of motion for which Eq. (1) holds.

We wonder now what would be the behavior of the electromagnetic radiation in the case when the dielectric has a cylindrical indefinite hole of radiation d parallel to the motion. This hole is necessary for the passage of intense beams. As first guess, if the hole is sufficiently small, it is an irrelevant perturbation for the Cerenkov radiation. Now, we must refine the concept of small or large hole. The particle sees the dielectric by means of its harmonic contents for those wavelengths such that

$$\lambda \geq d \tag{4}$$

So that Cherenkov radiation occurs only below certain frequencies (low pass filter behavior). So that, if the radius d is of the order of centimeter, we expect this will occur at frequencies of the order of GHz.

We understand also that radiation in the optical range is possible only if the dimensions of the hole are of the order of microns.

If in addition, the dielectric is limited and surrounded by an infinite metallic cylinder (**Figure 3**), becoming a partially loaded waveguide, we get a cutoff frequency, so the whole system behaves as passband filter.

A quantitative analysis can be conducted by using the mode expansion of the electromagnetic field in the waveguide matched to the Fourier expansion of the source current [6].

The configuration of this device gives an additional phenomenon, which can be exploited in the microwave range in order to enhance the intensity of radiation. In fact, the Cherenkov wave is trapped in the dielectric and therefore it is possible to pump power in it.

We can understand this trapping by considering the wave number in the dielectric and in the vacuo. They must satisfy the following triangular relations:

$$k_x^2 + k_y^2 + k_z^2 = k_0^2 \tag{5}$$

$$(k_x^d)^2 + k_y^2 + k_z^2 = n^2 k_0^2 \tag{6}$$

From Eqs. (5) and (6), taking into account that $k_x^d = nk_0 \sin \theta$, we have

$$k_x^2 = (1-n^2 \cos^2 \theta)k_0^2 \tag{7}$$

If relation (3) holds, k_x is pure imaginary. The wave is evanescent toward the vacuum. There is no power flux in the transverse direction because the wave in the dielectric is in condition of total reflection. The wave is trapped, because of the multiple reflections on the metallic walls and the interface between the dielectric and the vacuum. Accordingly, there is the possibility to increase the power flux with waves with an adequate phase relation among them when the particle beam has a sinusoidal density modulation.

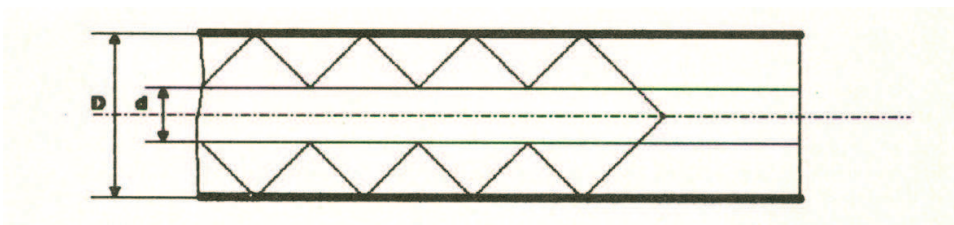


Figure 3. Cherenkov radiation in partially filled waveguide.

4. Cerenkov free-electron laser

Laboratories around the world have realized free-electron laser (FEL) sources, emitting in spectral regions where conventional laser sources are not easily available (e.g., UV, FIR, and millimeter-wave). FEL facilities have been realized in the United States, Japan, China, and Europe. The European FEL sources emit in complementary spectral regions and, altogether, cover a wide spectral range from the UV to the millimeter wave region. The region between 150 and 1 mm is particularly attractive, when continuous tunability and high brightness at the same time are allowed, because conventional laser sources usually do not satisfy these requirements. Small size, moderate cost FEL can be built at such wavelengths. There are a variety of phenomena that can be studied in this region in a solid-state and biological samples with

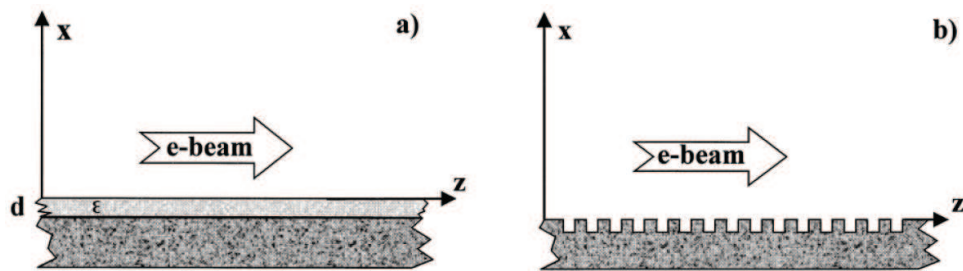


Figure 4. Coupling scheme for the C-FEL (a) and the G-FEL (b). The e-beam passes above the surface of a dielectric film, or of a metal grating, respectively, exciting TM-like surface waves.

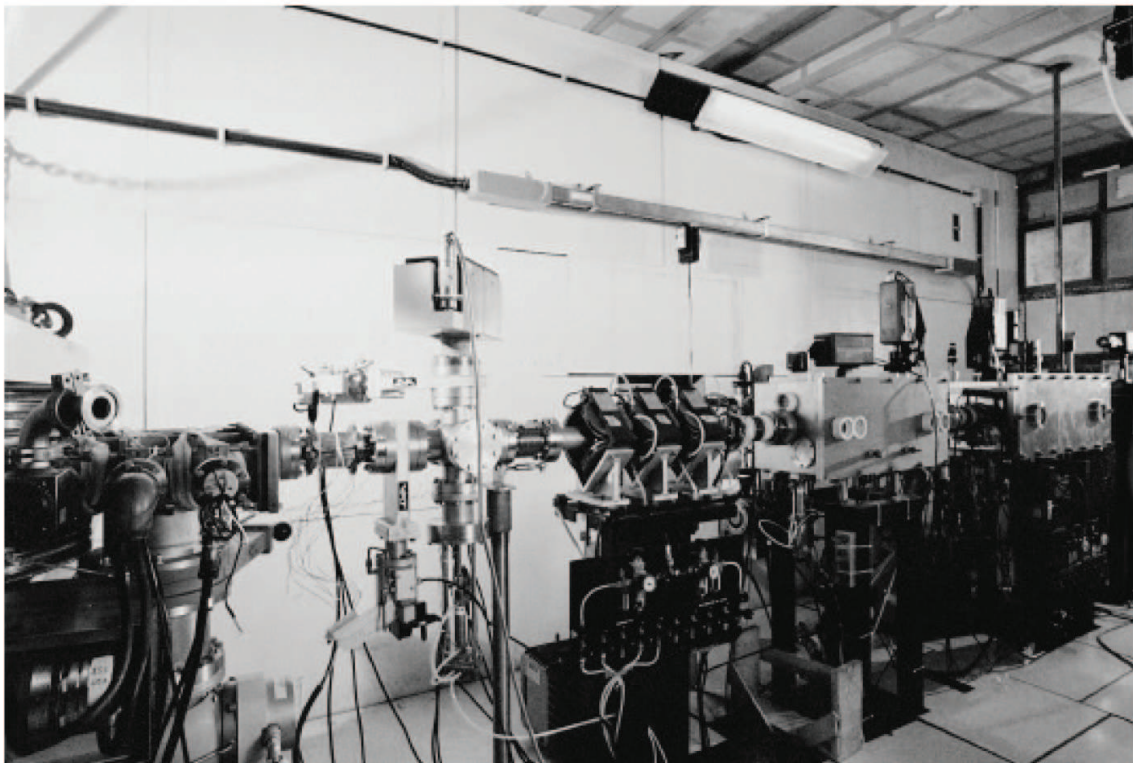


Figure 5. FEL facility developed at the ENEA Research Center in Frascati.

particular respect to their nonlinear response. Moreover, a FEL utilizing as a driver, a radio-frequency (RF) accelerator (**Figure 4**) is a unique source capable of providing picosecond pulses of coherent radiation at such wavelengths (**Figure 5**).

It is known [7] that the rate of energy exchange between flowing charges and a wave, **Figure 4**, is given by the integration of the product $\mathbf{J} \cdot \mathbf{E}$ over the volume of the region of space where the interaction occurs (Section 6).

The energy exchange will only occur between corresponding components of the electron current density and the wave electric field. In general, the longitudinal component of the current density due to the drift motion of the electrons will not couple to an electromagnetic wave propagating in the free space, since the latter one has zero longitudinal electric field component. However, in a waveguide or in a suitable loaded structure like the traveling wave tube (TWT) TM modes can be excited, which have a longitudinal component of the electric field. Cerenkov free-electron lasers and orotrons or grating rely on this type of coupling scheme [7].

In Section 6, a general theory is proposed to study the coupling between an electron beam and a hybrid waveguide.

5. Cherenkov imaging

When charged particles travel through dielectric media, such as biological tissue, faster than the speed of light, Cherenkov radiation exists.

Detection of this radiation can allow a new approach to superficial dose estimation, functional imaging, and quality assurance for radiation therapy dosimetry. The first *in vivo* Cherenkov images of a real-time Cherenkovscopy have been recently presented [8]. The imaging system consisted of a time-gated intensified charge coupled device (ICCD) coupled with a commercial lens. The ICCD was synchronized to the linear accelerator to detect Cherenkov photons only during the 3.25 μ s radiation bursts. Images of a tissue phantom under irradiation show that the intensity of Cherenkov emission is directly proportional to radiation dose.

Cherenkovscopy was obtained from the superficial regions of a canine oral tumor during planned, Institutional Animal Care and Use Committee approved, conventional (therapeutically appropriate) irradiation. Coregistration between photography and Cherenkovscopy validated that Cherenkov photons were detected from the planned treatment region. Real-time images correctly monitored the beam field changes corresponding to the planned dynamic wedge movement, with accurate extent of overall beam field, and expected cold and hot regions.

The experimental configuration is shown in **Figure 6**. The external beam irradiator was a Varian Clinic 2100CD linear accelerator (LINAC, Varian Medical Systems, Palo Alto, CA). A time-gated intensified charge coupled device (ICCD) camera was set up on a tripod to image the entrance region of the treatment beam on tissue phantoms or tissue. The LINAC delivers radiation in a pulsed mode and the ICCD camera was synchronized to the 3.25 μ s radiation bursts, detecting Cherenkov emission effectively and rejecting most of the ambient light. This

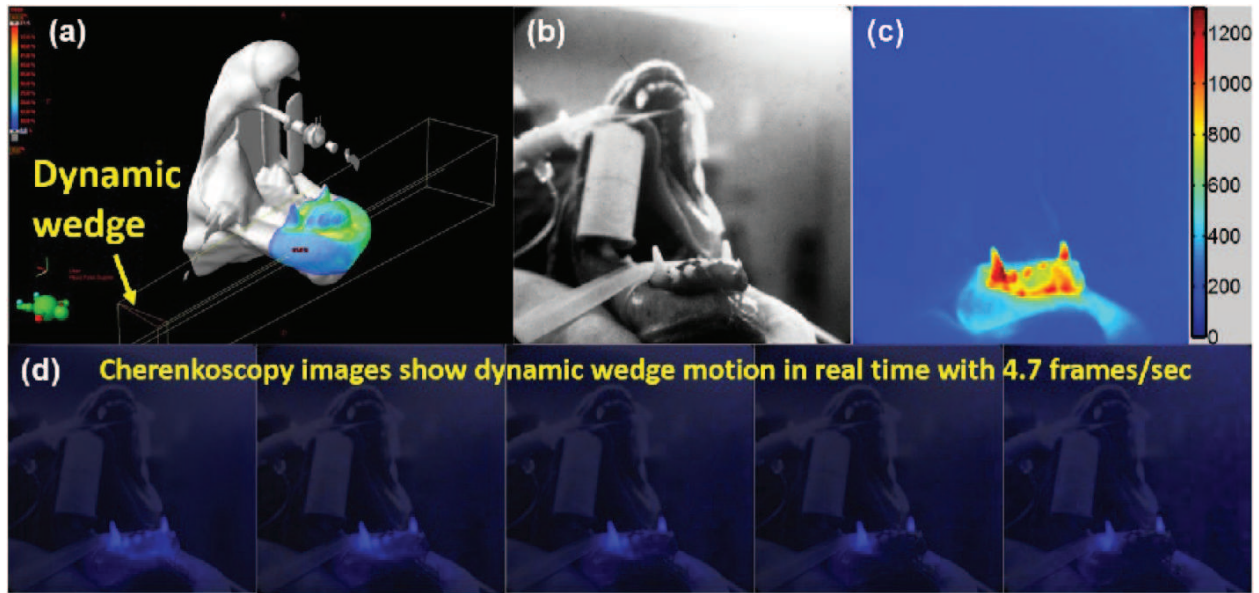


Figure 6. (a) The treatment plan shows incident of the beam and dynamic wedge. (b) Field view of the treatment region. (c) Cherenkov images of the treatment region while irradiation progresses. (d) Cherenkov images overlaid on the white-light images of the treatment field and sequence of Cherenkov images showing the beam field changing while a wedge is moved into the beam. From Ref. [8].

imaging system was first tested by imaging Cherenkov emission from a slab 30304 cm^3 phantom made of opaque water equivalent plastic while irradiating it with a 6 MV square 1010 cm^2 photon beam at a dose rate of 600 monitor units per minute. Cherenkov images for different delivered doses at d_{max} were acquired [8].

6. General pickup theory

The extension of stochastic cooling to SPS accelerator of CERN needs high sensitivity pickup (PU) and kickers. To achieve this goal the author, during a period spent a CERN, introduced a new class of pickup and kickers [9]: synchronous PU. The main concept is to use the synchronism between the beam and a slow wave propagating in a structure in which the phase velocity of the wave coincides with the beam velocity. In a metallic rectangular waveguide, the phase velocity is always larger than the velocity of light. However, if we change the *surface impedance* of two opposite walls of the guide slow waves (waves with a phase velocity lower than the velocity of light) propagate in the inhomogeneous waveguide. We have several possibilities to change the surface impedance. The following two solutions will be examined: dielectric slabs and metallic corrugation.

The modes propagating within an inhomogeneous waveguide are a combination of TE and TM modes (hybrid modes). They are classified [10] as LSE (longitudinal section electric) and LSM (longitudinal section magnetic). The component of the fields can be derived from scalar Hertzian potential: the electric type Π_E for LSM modes and the magnetic type Π_H for LSE modes.

The solution of the equation for the potential Π_E or Π_H is a superposition of an even and odd solution with respect to the transverse dimension. The odd solution for Π involves an even dependence of $E_{z(mn)}$ and suggests the use as a longitudinal pickup because the hybrid mode is excited by the beam placed in the center of the structure. On the other hand, the even solution for Π (odd for $E_{z(mn)}$) is excited when the beam is off-center in the waveguide and this suggests to use this solution for a transverse pickup.

6.1. The reciprocity theorem

To establish the fundamental relations between the input-output, we use a simple representation of the pickup, or kicker (**Figure 7**): a black box connected to the vacuum chamber where the beam circulates along the z-axis having an output port terminated by a matched load. For a given beam current traveling through the pickup, we want to calculate the complex voltage on the output termination.

The PU is divided into two parts:

- Synchronous part AA'-BB' where the phase velocity of the EM field is approximately the same as that of the particles.
- A transition part BB'-CC' where the EM field excited in AA'-BB' is transformed into a wave propagation in the output waveguide.

We assume that there is a perfect coupling that is all power flowing in the part AA'-BB' is transformed into power flowing into the output part. This means that no field propagates along the beam pipe. The coupling between the beam and the transition region where there is no synchronism is also neglected.

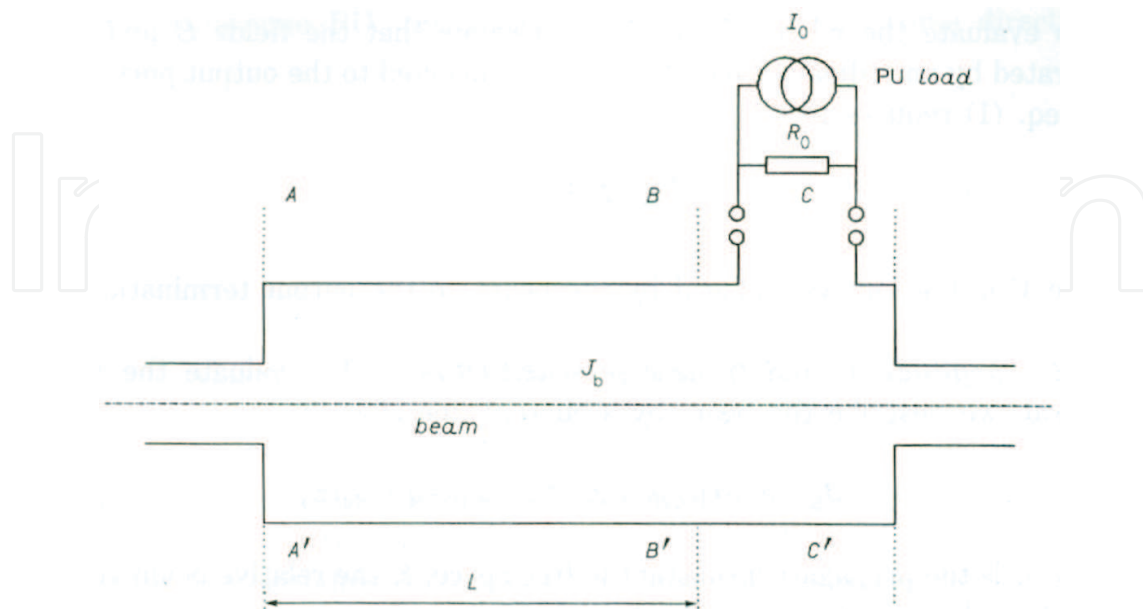


Figure 7. Pickup structure.

In order to apply the reciprocity theorem, we consider the electromagnetic fields \mathbf{E}_b and \mathbf{H}_b generated by the beam with a current density \mathbf{J}_b , and the fields \mathbf{E} and \mathbf{H} in the PU structure produced by another current source having a current density \mathbf{J} .

The Lorentz reciprocity theorem states

$$\oint_S (\mathbf{E}_b \times \mathbf{H} - \mathbf{E} \times \mathbf{H}_b) \cdot \hat{\mathbf{n}} ds = \iiint_V [\mathbf{E} \cdot \mathbf{J}_b - \mathbf{E}_b \cdot \mathbf{J}] dv \quad (8)$$

In Eq. (8), V is the volume enclosed by the surface S , where there is interaction between the beam and the slow wave structure, $\hat{\mathbf{n}}$ is the unity vector normal to S .

To evaluate the r.h.s. of Eq. (8) we assume that the fields \mathbf{E} and \mathbf{H} are generated by an ordinary current source I_0 connected to the output port. In this case, Eq. (8) reduces to

$$\iiint_V \mathbf{E} \cdot \mathbf{J}_b dv = I_0 V \quad (9)$$

where V is the voltage induced by the beam on the output termination R_0 .

6.1.1. Longitudinal and transverse sensitivities

To evaluate the volume integral, we describe the beam by a current line along z :

$$\mathbf{J}_b = J_b e^{\left[\frac{j k_0 z}{\beta_p} \right]} \delta(x-x_0) \delta(y-y_0) \hat{\mathbf{z}} \quad (10)$$

Where k_0 is the propagation constant in free space, β_p is the relative beam velocity, x_0 and y_0 are the transverse coordinates of the beam.

Assuming that the wave excited by I_0 in the structure is a pure traveling wave, of the form

$$E_z(x,y,z) = E_z(x,y) e^{\left[\frac{j k_0 z}{\beta_w} \right]} \quad (11)$$

β_w being its phase velocity, Eq. (9) transforms into

$$\frac{V}{I_b} = \frac{E_z(x_0, y_0)}{I_b} L \left| \text{sinc} \left\{ k_0 \frac{L}{2} \left(\frac{1}{\beta_p} - \frac{1}{\beta_w} \right) \right\} \right| \quad (12)$$

where L is the pickup length, I_b is the Fourier component of the beam current and sinc the $\sin x/x$ function.

This wave carries the power P_T given by

$$P_T = \frac{1}{2} \iint_{\Sigma} \mathbf{E} \times \mathbf{H}^* \cdot \hat{\mathbf{n}} d\Sigma \quad (13)$$

The current source I_0 , which generates P_T is split in two equal parts: $I_0/2$ flows into the PU load R_0 and $I_0/2$ in the PU itself. It follows:

$$P_T = \frac{1}{2} R_0 \left(\frac{I_0}{2} \right)^2 \quad (14)$$

In the longitudinal case, the PU sensitivity (or transfer impedance) defined as $S = V/I_b$ is obtained simply by combining Eqs. (12) and (13).

$$S = \frac{1}{2} \sqrt{\frac{R_0}{2P_T}} E_z(x_0, y_0) L \left| \text{sinc} \left\{ k_0 \frac{L}{2} \left(\frac{1}{\beta_p} - \frac{1}{\beta_w} \right) \right\} \right| \quad (15)$$

For a transverse PU, the sensitivity S_Δ , for the transverse direction x , is defined as

$$S_\Delta = \frac{1}{I_b} \frac{\partial V}{\partial x} \Big|_{x=x_0} \quad (16)$$

leads to

$$S_\Delta = \frac{1}{2} \sqrt{\frac{R_0}{2P_T}} \left[\frac{\partial E_z(x, y_0)}{\partial x} \right]_{x=x_0} L \left| \text{sinc} \left\{ k_0 \frac{L}{2} \left(\frac{1}{\beta_p} - \frac{1}{\beta_w} \right) \right\} \right| \quad (17)$$

We have to evaluate P_T using Eq. (14), for a given field supported by the structure. We consider an even mode, for E_z , in the case of a longitudinal PU and an odd mode for a transverse PU.

6.2. Kicker transfer functions

The force on a charge q , moving with the velocity $v = v\hat{z}$, in an electromagnetic field (\mathbf{E} , \mathbf{H})

$$\frac{d\mathbf{p}}{dt} = q\mathbf{E}(t) + q\mu_0 v (\hat{y}H_x(t) - \hat{x}H_y(t)) \quad (18)$$

Integrating along the kicker length L one obtains, in frequency domain,

$$\Delta\mathbf{p} = \frac{q}{v} \int_0^L [(\mathbf{E} + \mu_0 v (H_x \hat{y} - H_y \hat{x})) e^{j\frac{k_0 z}{\beta_p}}] dz \quad (19)$$

The projection of Eq. 19 along the z -axis

$$\Delta p_z = \frac{q}{V} \int_0^L E_z e^{j\frac{k_0 z}{\beta_p}} dz \quad (20)$$

gives the kicker transfer function in the longitudinal case.

To obtain the transverse sensitivity, the projection of Eq. (20) along the x -axis is considered



Figure 8. Dielectric pickup.

$$\Delta p_x = \frac{q}{v} \int_0^L \left[E_x - \frac{v}{j\omega} \left(\frac{\partial E_z}{\partial x} - \frac{\partial E_x}{\partial z} \right) \right] e^{j\frac{k_0}{\beta_p} z} dz \quad (21)$$

For a wave propagating along z , of the form $\exp\left[j\frac{k_0}{\beta_p} z\right]$, Eq. (20) gives

$$\Delta p_x = \frac{q}{v} \int_0^L \left[E_x \left(1 - \frac{\beta_p}{\beta_w} \right) + j \frac{\beta_p}{k_0} \frac{\partial E_z}{\partial x} \right] e^{j\frac{k_0}{\beta_p} z} dz \quad (22)$$

When $\beta_p = \beta_w$, i.e., at synchronism, the first term in the integral vanishes. Eqs. (22) and (17) are then essentially the same as well as Eqs. (13) and (8) for the longitudinal case. In conclusion, PU sensitivity and kicker transfer function are basically the same quantities, for a given geometry or, in other words as we can expect that kickers are essentially pickup structures working in reverse.

In **Figure 8** is presented a dielectric pickup developed a CERN from the author for the stochastic cooling of bunched beams in the SPS accelerator.

7. Corrugated waveguide

As example of waveguide supporting slow waves, we consider the corrugated waveguide depicted in **Figure 9**.

The electromagnetic field inside the waveguide, when we consider the hybrid longitudinal section electric (LSE) mode, can be described by the Hertzian potential

$$\mathbf{\Pi}^H = \hat{\mathbf{x}} P(x,y) e^{\gamma_n z} \quad (23)$$

$$\mathbf{E} = -j\omega\mu_0 \nabla \times \nabla \times \mathbf{\Pi}^H \quad (24)$$

$$\mathbf{H} = \nabla \times \mathbf{\Pi}^H \quad (25)$$

The solution of Eqs. (23)–(25) gives the field components:

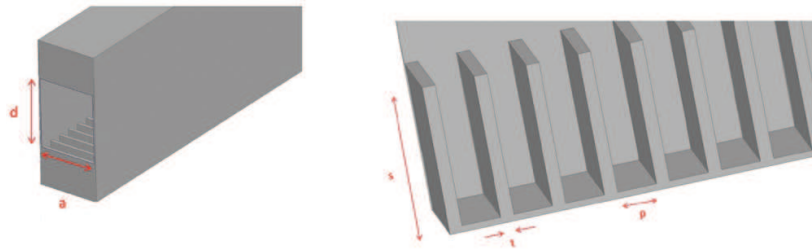


Figure 9. Geometry of corrugated waveguide.

$$e_x = 0 \quad (26)$$

$$e_y = -\omega\mu_0\gamma_n P(x,y) \quad (27)$$

$$e_z = -j\omega\mu_0 \frac{\partial}{\partial y} P(x,y) \quad (28)$$

$$h_x = -\left(\frac{\partial^2}{\partial y^2} + \frac{\partial^2}{\partial z^2}\right) P(x,y) \quad (29)$$

$$h_y = \frac{\partial^2}{\partial x \partial y} P(x,y) \quad (30)$$

$$h_z = -j\gamma_n \frac{\partial}{\partial x} P(x,y) \quad (31)$$

$$k_0^2 = \gamma_n^2 + k_x^2 + \alpha^2 \quad (32)$$

Inside the corrugation, we have

$$E_z = -j\omega\mu_0 B \sin \beta \left(\frac{d}{2} + s - y\right) \cos \frac{\pi}{a} x \quad (33)$$

$$H_y = \frac{\pi}{a} B \sin \beta \left(\frac{d}{2} + s - y\right) \sin \frac{\pi}{a} x \quad (34)$$

$$H_x = -\beta B \cos \beta \left(\frac{d}{2} + s - y\right) \cos \frac{\pi}{a} x \quad (35)$$

The dispersion equation inside the corrugation gives

$$k_0^2 = \beta^2 + k_x^2 \quad (36)$$

Eqs. (32) and (36) give

$$\beta^2 = \gamma_n^2 + \alpha^2 \quad (37)$$

Expression (37) for slow waves ($\alpha = jq$) becomes

$$\beta^2 = \gamma_n^2 - q^2 \quad (38)$$

The general solution of the potential equation is a superposition of an even and an odd solution, with respect to ($y = 0$). For the even solution, we have

$$P(x,y) = A \cos\left(\frac{n\pi}{a}x\right) \cosh(qy) \quad (39)$$

Imposing the boundary condition for the field (Eq. (24)) on the air-corrugation interface:

$$e_z\left(\frac{d}{2}, x\right) = E_z\left(\frac{d}{2}, x\right) \quad (40)$$

$$h_x\left(\frac{d}{2}, x\right) = H_x\left(\frac{d}{2}, x\right) \quad (41)$$

the following transcendental equation is obtained

$$\frac{1}{\alpha} \tan \alpha \frac{d}{2} = \frac{1}{\beta} \cot \beta s \quad (42)$$

In the slow wave case ($\alpha = jq$), we have

$$\tanh q \frac{d}{2} = \frac{q}{\beta} \cot \beta s \quad (43)$$

The solution of Eqs. (42) and (38) gives the dispersion equation of waveguide.

8. Waveguide pulse compression

Pulsed radars can achieve high-resolution range using pulses with a very short duration. The maximum range for the system requires a fixed pulse repetition rate that represents a reduction of mean power unless there is an increment of the peak power. A limit to the peak power is imposed by transmitter components, so an attractive alternative consists in the use of f.m. pulse-compression techniques.

Passive compressors for pulse consist of a passive circuit with frequency dispersion with a phase-modulated input pulse.

As dispersive circuit, one can use a section of metallic waveguide in which group velocities depend on the frequency. Thus, if the input microwave pulse is frequency modulated, each component of the pulse travels with its velocity. With a linear growing frequency, one can obtain a situation such that all parts of the pulse simultaneously arrive at the waveguide output.

Standard metallic waveguides are strongly dispersive near the cutoff frequency which limits the use to low power levels with short input pulse durations. More sophisticated waveguide

can be used for better performance. The corrugated waveguide, where it is possible to excite a slow wave, is a good candidate.

9. Slow wave compressor

From Eq. (38), the propagation constant in the corrugated waveguide is found as

$$\gamma_n^2 = \beta^2 + \frac{12}{d^2} - \frac{24}{\beta d^3} \cot \beta s \quad (44)$$

From Eq. (44), it is possible to find the group velocity

$$v_g = \frac{\partial \omega}{\partial \gamma_n} \quad (45)$$

We use modulated pulse with a linear swept frequency that monotonically increasing group velocity propagating through the waveguide. This results in pulse shortening and growth in power amplitude if the losses are small. The maximum compression ratio is obtained at the exit of the waveguide where all the frequency components of the pulse arrive at the same time. The compression ratio is derived from the electromagnetic wave propagating along an isotropic dispersive medium

$$K = \Delta FL \left(\frac{1}{v_{g1}} - \frac{1}{v_{g2}} \right) e^{-\delta L} \quad (46)$$

Where v_{g1} and v_{g2} are the group velocity of the beginning and the end frequencies of the microwave pulse, L is the length of waveguide, ΔF is the frequency band, and δ is the loss factor.

Dispersion relation, group velocity, and compression ratio of a typical slow wave waveguide are reported in **Figures 10–12**.

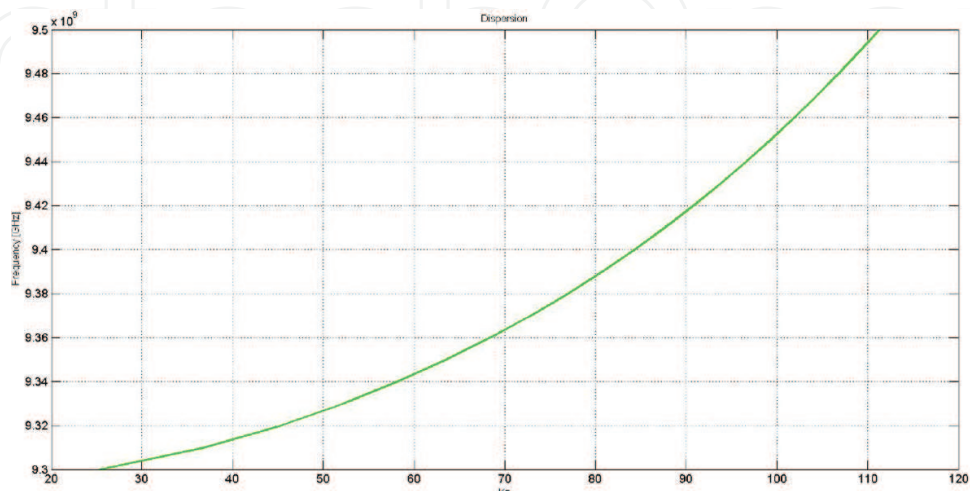


Figure 10. Dispersion of corrugated waveguide.

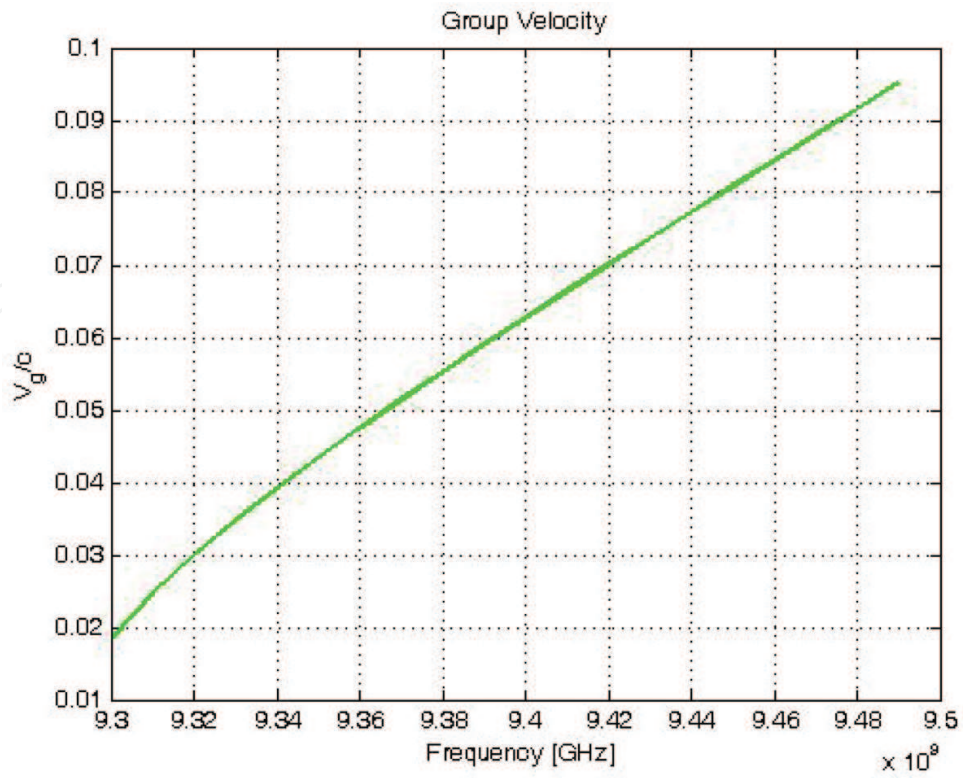


Figure 11. Group velocity of corrugated waveguide.

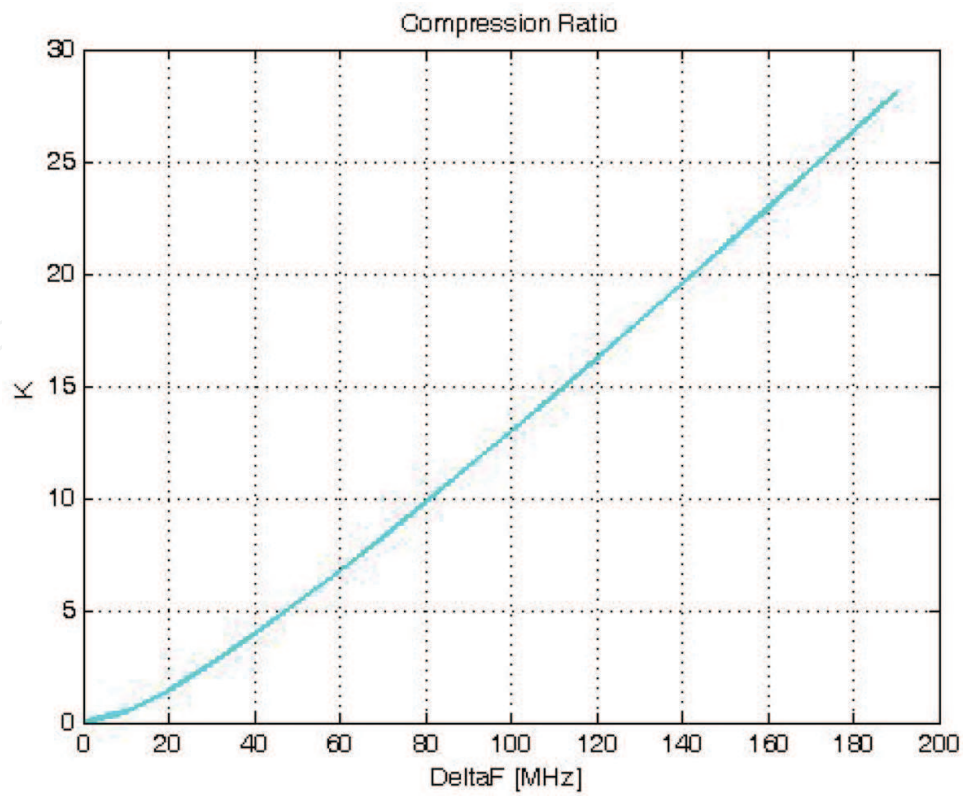


Figure 12. Compression ratio of corrugated waveguide.

10. Compact components and waveguide in microwave region

A slow-wave coplanar waveguide transmission lines, combining the advantages of both coplanar transmission lines and microstrip lines, is reported [11] to create high-performance passive components for millimeter wave integrating circuits. To achieve a slow wave, periodical slot-type floating shields are used to enable a reduction in a chip area while still maintaining high performance. Slot-type floating shields also enhance the immunity of slow-wave CPW transmission lines from ac noise (**Figure 13**).

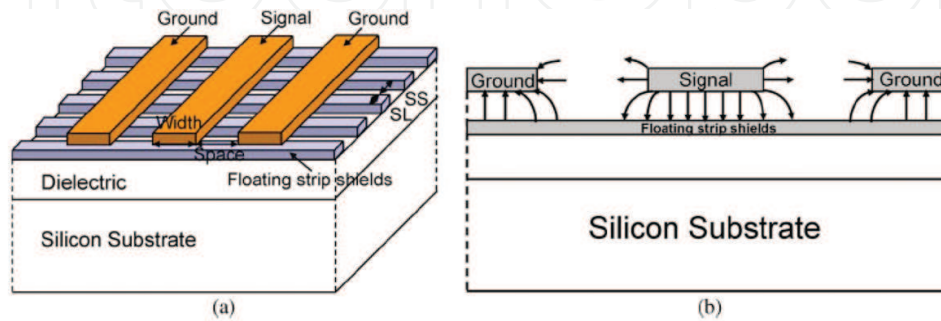


Figure 13. Slow-wave coplanar waveguide transmission line with slot-type floating shields. (a) Schematic view and (b) electric field distribution from 3-D EM simulation. From Ref. [11].

If the length of the periodical structure is short compared to the wavelength, each segment of signal line can be modeled by an inductance and capacitance lumped-element equivalent circuit, where L and C are the series inductance and the shunt capacitance per unit length, respectively. The density R of the slot-type floating shields is defined as

$$R = \frac{SL}{SL + SS} \quad (47)$$

Consequently, the phase velocity V_p with the slow-wave effect can be expressed as

$$V_p = \frac{1}{\sqrt{LC(nR)}} \quad (48)$$

where n represents the increased ratio in capacitance as a result of coupling to the slot-type shields. The slow-wave phenomenon can be explained in Eq. (48), which shows that the phase velocity is decelerated by a factor of \sqrt{nR} .

11. Conclusions

The chapter reports some applications of the interaction of slow electromagnetic waves with dielectric or corrugated media. The thread through the chapter is the possibility of generating electromagnetic waves from traveling particles in the considered medium or, vice versa, the

possibility to influence the motion of particles. An extension of this approach is the possibility of compressing the fields for applications in radars and linacs or to think about microwave devices and antennas of reduced dimensions for integration in the active circuits.

Author details

Giuseppe Di Massa

Address all correspondence to: dimassa@deis.unical.it

University of Calabria, Italy

References

- [1] P. A. Cerenkov, Visible emission of clean liquids by action of γ radiation C. R. Acad. Sci. USSR, **8**, 451,1934.
- [2] Cerenkov P A, Visible radiation produced by electrons moving in a medium with velocities exceeding that of light, Phys. Rev. **52**, 378, 1937.
- [3] I. Frank, I. Tamm, Coherent visible radiation from fast electrons passing through matter, C. R. Acad. Sci. USSR, **14**, No. 3, 1937.
- [4] J. V. Jelley, *Cerenkov radiation and its applications*, Br. J. Appl. Phys., **6**, 227, 1955.
- [5] G. Di Massa, V. G. Vaccaro, *Cerenkov Pick-up in the Microwave Band*, Hadronic Physic at Intermediate Energy, Elsevier Science Publishers, North Holland, Amsterdam, pp. 455–463, 1986.
- [6] H. L. Andrews, C. A. Brau, *Three-Dimensional Theory of the Cerenkov Free-Electron Laser*, Proc. of FEL 2007, Novosibisk, Russia.
- [7] G. P. Gallerano, A. Doria, E. Giovenale, A. Renieri, Compact free electron lasers: From Cerenkov to waveguide free electron lasers, Infrared Phys. Technol., **40**, 1999.
- [8] R. Zhang, D. J. Gladstone, L. A. Jarvis, R. R. Strawbridge, P. J. Hoopes, O. D. Friedman, A. K. Glaser, B. W. Pogue, *Real-time in vivo Cherenkovscopy imaging during external beam radiation therapy*, J. Biomed. Opt., **11**, 2013.
- [9] G. Di Massa, *High frequency slow wave pick-ups for stochastic cooling of bunched beams*, II Nuovo Cimento, **100**, 1988.
- [10] R. E. Collin, *Field Theory of Guided Waves*, McGraw Hill, N. Y., 1960, IEEE Trans. Plasma Sci., **30**, No. 3, 755–786, 2002.
- [11] Hsiu-Ying Cho, Tzu-Jin Yeh, Sally Liu, and Chung-Yu Wu, *High-performance slow-wave transmission lines with optimized slot-type floating shields*, IEEE Trans. Electron Dev., **56**, 2009.